

Huxley equations for squid axon treated with tetraethylammonium and in potassium rich media," *Austral. J. Exp. Biol. Med. Sci.*, vol. 39, pp. 275-293, 1961.

[21] F. A. Dodge, "Ionic permeability changes underlying nerve excitation," in *Biophysics of Physiological and Pharmacological Actions*, Amer. Assoc. Advan. Sci., Washington, D.C., pp. 113-143, 1961.

[22] B. Frankenhauser and A. F. Huxley, "The action potential in the myelinated nerve fibre of *Xenopus laevis* as computed on the basis of voltage clamp data," *J. Physiol.*, vol. 171, pp. 302-315, 1964.

[23] B. Frankenhauser and A. B. Vallbo, "Accommodation in myelinated nerve fibers of *Xenopus laevis* as computed on the basis of voltage clamp data," *Acta Physiol. Scan.*, vol. 63, pp. 1-20, 1965.

[24] A. J. Brady and J. W. Woodbury, "The sodium-potassium hypothesis as the basis of electrical activity in frog ventricle," *J. Physiol.*, vol. 154, pp. 385-407, 1960.

[25] R. E. McAllister, D. Noble, and R. W. Tsien, "Reconstruction of the electrical activity of cardiac Purkinje fibres," *J. Physiol.*, vol. 251, pp. 1-59, 1975.

## Short Papers

### Easy Determination of the Characteristic Impedance of the Coaxial System Consisting of an Inner Regular Polygon Concentric with an Outer Circle

KOICHI TSURUTA AND RYUITI TERAKADO

**Abstract**—This paper gives a simple method for the determination of the characteristic impedance of an inner regular polygon concentric with an outer circle. The approach makes use of the method of superposition for plane sheets of charge which were radially disposed in the polygon. The results are in good agreement with those obtained by Laura and Luisoni [2], [3].

Riblet [1] and Laura and Luisoni [2], [3] have developed interesting techniques for the determination of the characteristic impedance of the coaxial system consisting of a regular polygon concentric with a circle. This paper gives a simpler method for an inner regular polygon of  $s$  apexes concentric with an outer circle.

An infinitely long conducting plane sheet of width  $2b$  charged with charge density  $Q$  per unit length in the  $z$  direction is situated in free space with permittivity  $\epsilon_0$ , as shown in Fig. 1. Suppose that the reference point for potential is at the conducting sheet whose potential is defined as  $A$ . The potential  $V_P$  at a point  $P(x, y)$  on the  $z$  plane can be obtained by conformal mapping of the  $z$  plane on a  $w$  plane, whose mapping function is

$$Z = \frac{b}{2} \left( w + \frac{1}{w} \right) + (c + ia). \quad (1)$$

By this mapping, equipotential lines on the  $w$  plane becomes concentric circles. Therefore, the potential  $V_P$  is easily written as follows:

$$V_P = A - \frac{Q}{2\pi\epsilon_0} \ln \left\{ \frac{\sqrt{\left(\frac{x-c}{b} - 1\right)^2 + \left(\frac{y-a}{b}\right)^2} + \sqrt{\left(\frac{x-c}{b} + 1\right)^2 + \left(\frac{y-a}{b}\right)^2}}{2} \right. \\ \left. + \sqrt{\left(\frac{x-c}{b}\right)^2 + \left(\frac{y-a}{b}\right)^2 - 1} + \sqrt{\left\{ \left(\frac{x-c}{b}\right)^2 + \left(\frac{y-a}{b}\right)^2 + 1 \right\}^2 - 4\left(\frac{x-c}{b}\right)^2} \right\} \quad (2)$$

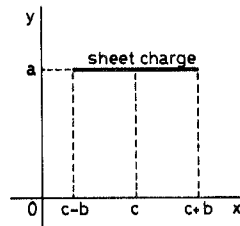


Fig. 1. Dimensions of the plane sheet of charge.

The electric field produced by the conducting sheet charge is derivable as the negative gradient of the potential.

In the proposed method an important supposition is made, that is, the distribution of charge on the conducting sheet invariably remain, even if other conducting sheets are set near it.

Fig. 2 shows the disposition of the sheets of charge for  $s = 5$ , for example. They were radially disposed between the center and the apexes of the polygon. The potential and the field at any point can be calculated analytically by superposition for these sheets of charge. The potentials at the sides of the polygon and at the outer circle were calculated for  $s = 3, 4, 5$ , and 6. Table I shows the maximum deviations of the potentials at the sides of the polygon and at the outer circle from the average potentials  $V_{\text{polygon}}$  and  $V_{\text{circle}}$ , respectively, expressed as percentages of the average potentials.  $V_{\text{polygon}}$  was calculated from the potentials at 100 points which were arranged on the half-side  $P_1 P_2$  (Fig. 2) at equal distances and were weighted by the field strength.  $V_{\text{circle}}$

Manuscript received December 4, 1978; revised June 13, 1979.  
The authors are with the Department of Electrical Engineering, Ibaraki University, Hitachi Ibaraki, 316 Japan.

was calculated in the same manner as  $V_{\text{polygon}}$  from the potentials on the arc  $C_1 C_2$ .  $R$  is the radius of the circle and  $r$  is the radius of the circumscribed circle of the polygon.

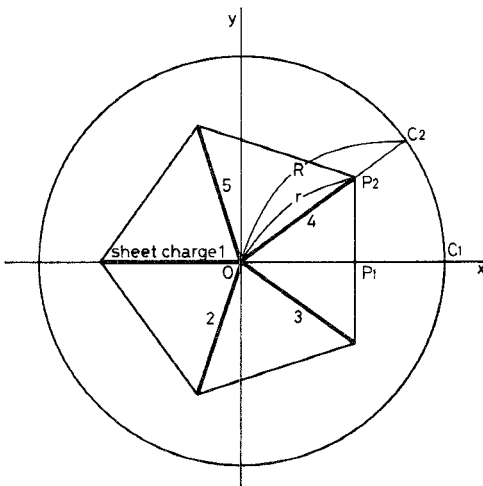
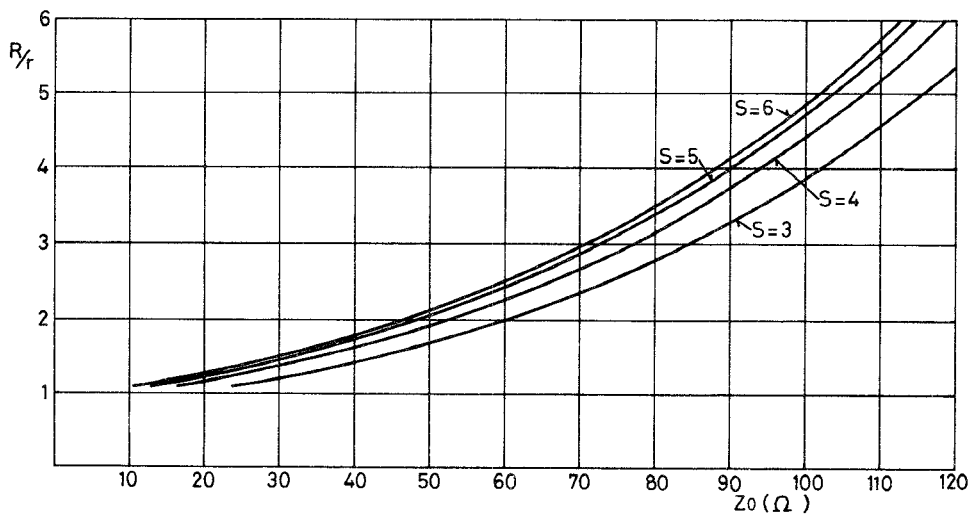
Fig. 2. Disposition of the plane sheets of charge for  $s=5$ .Fig. 3. Characteristic impedances for  $s=3, 4, 5$ , and  $6$ .

TABLE I

THE MAXIMUM DEVIATIONS OF THE POTENTIALS AT THE SIDES OF THE POLYGON AND AT THE OUTER CIRCLE FROM THE AVERAGE POTENTIALS  $V_{\text{polygon}}$  and  $V_{\text{circle}}$ , RESPECTIVELY, EXPRESSED AS PERCENTAGES OF THE AVERAGE POTENTIALS

s		3	4	5	6
at the polygon		6.67%	2.36%	1.07%	1.23%
at the circle R/r	1.2	4.70%	2.46%	1.43%	0.89%
	1.4	2.44	1.11	0.56	0.30
	1.6	1.46	0.58	0.26	0.12
	1.8	0.94	0.34	0.13	0.06
	2.0	0.64	0.21	0.07	0.03

Further, it was found that the deviation of the potential at the sides of the polygon could be reduced by the adjustment of the width of the sheets. The width of the sheets was adjusted at intervals of 0.1 percent of the first width to find the most suitable width of the sheets of charge which minimize the deviation of the potential at the sides of the polygon. In this adjust-

TABLE II

THE MOST SUITABLE WIDTH OF SHEETS OF CHARGE AND THE MAXIMUM DEVIATIONS OF THE POTENTIALS AT THE SIDES OF THE POLYGON AND AT THE OUTER CIRCLE

s		3	4	5	6
width of the sheets		74.4%	85.6%	98.5%	112.4%
at the polygon		1.05%	1.17%	1.00%	0.85%
at the circle R/r	1.1	7.10%	4.06%	2.61%	1.81%
	1.2	4.67	2.44	1.43	0.90
	1.4	2.48	1.11	0.56	0.30
	1.6	1.51	0.59	0.26	0.12
	1.8	0.98	0.34	0.13	0.06
	2.0	0.68	0.21	0.07	0.03
2.5		0.31	0.08	0.02	0.01
3.0		0.17	0.04	0.01	0.00
3.5		0.10	0.02	0.00	0.00
4.0		0.06	0.01	0.00	0.00

ment, one edge of the sheets were fixed at the apexes of the polygon and the width was adjusted at the inner edges. As the result of the adjustment, the width of the sheets was reduced for  $s = 3, 4$ , and  $5$ , and stretched for  $s = 6$ . Therefore, the sheets were separated at the center of the polygon for  $s = 3, 4$ , and  $5$ , and were overlapped for  $s = 6$ .

Table II shows the most suitable width of the sheets of charge which were expressed as the percentage of the first width and the maximum deviations of the potentials at the sides of the polygon and at the outer circle after the adjustment. The Table II shows that the sides of the polygon could be considered to be equipotential with error of about 1 percent for  $s = 3, 4, 5$ , and  $6$ . The outer circle could be considered to be equipotential too, with error which were depended on  $s$  and  $R/r$ . Then the characteristic impedance of the coaxial system of an inner regular polygon concentric with an outer circle can be calculated from the approximate capacitance of the system per unit length. This is given by

$$C = \frac{sQ}{V_{\text{polygon}} - V_{\text{circle}}}. \quad (3)$$

Fig. 3 shows the numerical results for the characteristic impedance as a function of  $R/r$ . The results by this method are in good agreement with those obtained by Laura and Luisoni [2], [3].

#### REFERENCES

- [1] H. J. Riblet, "An accurate determination of the characteristic impedance of the coaxial system consisting of a square concentric with a circle," *IEEE Trans. Microwave Theory Tech.*, vol. MTT-23, pp. 714-715, Aug. 1975.
- [2] P. A. A. Laura and L. E. Luisoni, "Approximate determination of the characteristic impedance of the coaxial system consisting of a regular polygon concentric with a circle," *IEEE Trans. Microwave Theory Tech.*, vol. MTT-25, pp. 160-161, Feb. 1977.
- [3] —, "An application of conformal mapping to the determination of the characteristic impedance of a class of coaxial systems," *IEEE Trans. Microwave Theory Tech.*, vol. MTT-25, pp. 162-163, Feb. 1977.

### A K-Band Ruby Maser with 500-MHz Bandwidth

CRAIG R. MOORE

**Abstract**—Engineering improvements to a previously described reflected-wave maser design have resulted in an instantaneous 3-dB bandwidth of 400 MHz at 19.5 GHz, increasing to 560 MHz at 24 GHz. Nominal gain is 27 to 31 dB and gain flatness is  $\pm 2.5$  dB over this tuning range. Noise temperature variation across the passband is less than  $\pm 1.5$  K and the effective noise temperature referred to the room temperature input flange ranges from  $9.5 \pm 4$  K to  $13.5 \pm 4$  K over the 18.5- to 25-GHz tuning range.

#### INTRODUCTION

We recently described a reflected-wave ruby maser for 18.3- to 26.6-GHz operation [1]. The purpose of this communication is to report the results of engineering improvements to this design which enable achievement of the full gain-bandwidth potential.

Manuscript received June 13, 1979.

The author is with the National Radio Astronomy Observatory, P. O. Box 2, Green Bank, WV 24944.

Five masers have now been constructed, with each unit showing improved performance over the previous one. The performance of the most recently constructed unit is described here.

As reported previously, the areas requiring attention were the impedance match between the circulator and ruby-filled waveguide, the cancellation of ripple in pairs of stages by appropriate phasing and the magnetic field fringing at the open ends of the superconducting magnet. Each of these areas has been improved, thus allowing substantial improvement in amplifier performance, with no changes to the basic design. Additionally, the input waveguide was modified to reduce the noise temperature.

#### ENGINEERING IMPROVEMENTS

The first area of improvement was the circulator impedance match. A nickel-cobalt ferrite was substituted for the nickel-zinc ferrite employed previously. Using the same circulator configuration and identical alumina matching pieces in the center of each waveguide arm, a 3 to 4 dB improvement in return loss was achieved, lowering the VSWR to below 1.15 in the center 1/3 of the waveguide band. However, the larger physical size of the ferrite disks results in appreciable moding loss at the high end of the band, thus reducing the upper tuning limit of the maser to 25.2 GHz. The improvement in gain ripple made this an acceptable trade-off.

The next significant improvement was separating the circulator block and maser structure into two units in order to permit measurement of the impedance match and delay at this critical junction. Phasing of ruby pairs for ripple cancellation was adjusted to within  $\pm 10^\circ$  over most of the waveguide band. Two methods were utilized to change the electrical length of a ruby. The direct approach is to cut a section off the pump end of the ruby bar. The alternate approach involves making the ruby slightly smaller in height and thus slightly increasing the cutoff frequency of the ruby-filled guide. Either technique gives acceptable results, but phase changes of more than one wavelength are more easily accomplished by reducing the ruby length.

Fringing at the open ends of the superconducting magnet results in a nonuniform field that reduces the useful length of the magnet. The direct solution to the problem was to add 5.1 cm to the magnet length and locate the ruby (approximately 15 cm long) equidistant from the ends of the magnet, which is now 20.3 cm long. When fitted with iron compensation shims a linear magnetic field taper of 225 G over 14.5 cm was obtained. This satisfied the theoretical requirements for achieving 500-MHz bandwidth and 40-dB electronic gain at 22 GHz.

#### MEASUREMENT TECHNIQUES

Measurements were performed with the maser and superconducting magnet mounted on a closed cycle helium refrigerator which maintained a physical temperature of 4.6 K. The maser pump source was a Siemens RWO 50 backward wave oscillator with output power in excess of 150 mW from 39 to 51 GHz. The pump transitions are not saturated at full bandwidth. A 4 to 5 dB increase in gain was noted when the pump power spectral density was doubled by reducing the pump FM deviation (electronic reduction to half-bandwidth). The full bandwidth gain/pump power sensitivity of 1.5 dB/dB is only 50 percent larger than the 1 dB/dB value obtained with the maser of [1]. Since the complete receiver employing that unit achieves a gain stability of